Probing energy transfer events in the light harvesting complex 2 (LH2) of *Rhodobacter sphaeroides* with two-dimensional spectroscopy

Andrew F. Fidler,[1] Ved P. Singh,[1] Phillip D. Long,[2] Peter D. Dahlberg,[2] and Gregory S. Engel[1,a)]

[1]*Department of Chemistry, The Institute for Biophysical Dynamics, and The James Franck Institute, The University of Chicago, Chicago, Illinois 60637, USA*

[2]*Graduate Program in the Biophysical Sciences, The University of Chicago, Chicago, Illinois 60637, USA*

(Received 17 August 2013; accepted 25 September 2013; published online 15 October 2013)

Excitation energy transfer events in the photosynthetic light harvesting complex 2 (LH2) of *Rhodobacter sphaeroides* are investigated with polarization controlled two-dimensional electronic spectroscopy. A spectrally broadened pulse allows simultaneous measurement of the energy transfer within and between the two absorption bands at 800 nm and 850 nm. The phased all-parallel polarization two-dimensional spectra resolve the initial events of energy transfer by separating the intra-band and inter-band relaxation processes across the two-dimensional map. The internal dynamics of the 800 nm region of the spectra are resolved as a cross peak that grows in on an ultrafast time scale, reflecting energy transfer between higher lying excitations of the B850 chromophores into the B800 states. We utilize a polarization sequence designed to highlight the initial excited state dynamics which uncovers an ultrafast transfer component between the two bands that was not observed in the all-parallel polarization data. We attribute the ultrafast transfer component to energy transfer from higher energy exciton states to lower energy states of the strongly coupled B850 chromophores. Connecting the spectroscopic signature to the molecular structure, we reveal multiple relaxation pathways including a cyclic transfer of energy between the two rings of the complex.
 [http://dx.doi.org/10.1063/1.4824637]

I. INTRODUCTION

Light harvesting complexes act as solar concentrators by increasing the cross-sectional area of the photosynthetically active region of the cell by transferring the excitation energy to nearby reaction centers, where charge separation ensues.[1–3] The light harvesting complex 2 (LH2) from the purple bacteria *Rhodobacter sphaeroides* is a peripheral antenna complex. Structurally, the complex consists of nine dimeric apoproteins which assemble into a ring-like structure with C_9 symmetry, shown in Figure 1.[4] The protein matrix binds two rings of bacteriochlorophyll a (BChl) chromophores, consisting of nine and eighteen chromophores respectively, held between two sets of alpha helices which span the lipid membrane *in vivo*. The larger of the two rings of chromophores is comprised of nine weakly interacting chromophores which absorb in the near infrared around 800 nm and are referred to as the B800 chromophores. The inner ring is comprised of 18 strongly interacting chromophores which principally absorb around 850 nm and are collectively referred to as the B850 chromophores. Higher lying excitations of the B850 chromophores also absorb at 800 nm and the high energy tail in the absorption spectrum around 770 nm can be attributed purely to excitations of the B850 chromophores.[5] The higher lying excited states are referred to as the B850* states. Nine carotenoid chromophores are intertwined through the protein complex, acting as both a structural linker and excitation donor to the bacteriochlorophyll chromophores.[4,6] LH2 complexes from different species exhibit similar molecular structures, though the number of subunits can vary.[7] The family of LH2 complexes can largely be categorized into two groups based on the number of chromophores: species like *Rhodopseudomonas acidophila* (27 BChl in a C_9 symmetric arrangement) and species like *Rhodospirillum molischianum* (24 BChl in a C_8 symmetric arrangement).[8] The *Rhodobacter sphaeroides* species studied here falls into the first category.

The electronic structure and dynamics of excitations in LH2 complex have been extensively studied by a variety of methodologies.[9–12] Excitation of the strongly coupled B850 pigments results in delocalized collective excitations that span three to four pigments several picoseconds following excitation.[13–16] Due to the in-plane arrangement of chromophores, most of the oscillator strength of the B850 excitations is concentrated in the lower energy states around 850 nm.[5] The electronic structure of the B800 chromophores is in some ways more complicated, since the homogeneous line width, energetic disorder, and inter-pigment couplings are all of the same order of magnitude.[17,18] Additionally, the higher energy B850* states can potentially mix with the B800 states,[19,20] and such mixed states have been proposed to be directly involved in the first energy transfer step between the two rings.[21] Energy transfer between the two rings occurs on a 700 fs timescale at room temperature.[22,23] Energy transfer from the carotenoids to the bacteriochlorophylls has been measured to proceed on a 50 fs timescale through a variety

a)Author to whom correspondence should be addressed. Electronic mail: gsengel@uchicago.edu

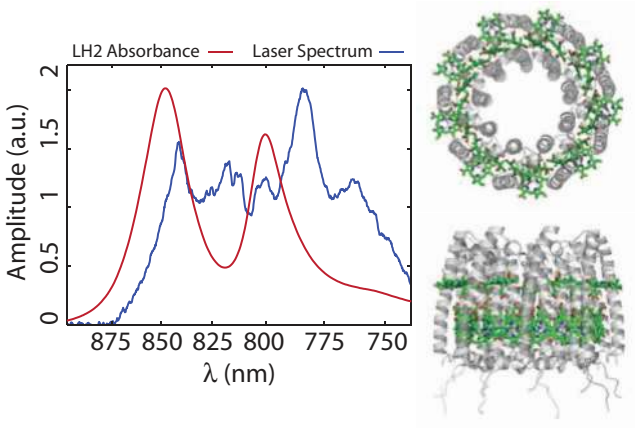

FIG. 1. The linear absorbance spectrum of LH2 (red) from *R. sphaeroides* shows two bands in the near infrared. The band at 850 nm and shoulder at 770 nm can largely be attributed to the B850 chromophores. The shoulder consists mainly of higher energy B850 states referred to as B850* states, while the feature at 800 nm is largely comprised of excitations on the B800 chromophores. The spectrally broadened pulse covers most of the absorption spectrum (blue). The crystal structure of LH2 is also shown for reference.

of different states.[24,25] Due to the relatively large inhomogeneity and high density of electronic states, the relaxation dynamics exhibit a strong wavelength dependence.[26] Competing pathways of energy transfer within the B800 chromophores as well as energy transfer from the higher energy B850 states into the B800 chromophores have been investigated.[22,27–32] Reduced density matrix calculations, utilizing a Redfield theory framework, can simultaneously reproduce the wavelength dependent transient absorption kinetics, absorption spectrum, and transient absorption anisotropy measurements.[19] Within this model the various time scales of energy transfer within and between the two rings can be inferred, providing a detailed picture of all the relaxation pathways. The model suggests that B800–B800 energy transfer is significantly slower than competing B800–B850* and B800–B850 relaxation pathways.

Experimentally probing energy transfer events in the LH2 complex is frustrated by the large density of states and broad resonances. Two-dimensional spectroscopy can improve resolution by spreading molecular information onto a two-dimensional map. Cross peaks on this map signify energy transfer events and arise from incomplete cancellation between ground state bleach and stimulated emission signals.[33] The appearance of energy transfer peaks is particularly useful for inhomogeneous systems, in which transitions between states within broad absorption bands can be difficult to probe with lower dimensional methods due to broad line widths and spectral features from excited state absorption.[25,34,35]

The inclusion of polarization control into two-dimensional spectroscopy can allow particular aspects of the relaxation dynamics to be isolated or highlighted.[36,37] Weak cross peaks resulting from couplings between chromophores can be directly isolated to provide a more accurate measurement of the couplings and energy transfer pathways in multichromophoric systems.[38–41] Comparisons between different polarization sequences, when combined with theoretical models, can help elucidate the structural arrangements of constituent chromophores.[42–44] Coherent contributions to the response, which report on time scales of dephasing of coherence among excited states, can also be isolated through control of the polarization.[20,45,46] Here, we present polarization controlled two-dimensional spectroscopy experiments designed to highlight initial energy transfer events,[36] along with all-parallel polarization experiments, on light harvesting complex 2 from *R. sphaeroides*. These experiments allow direct measurement of the initial energy transfer events. The details of the all-parallel and polarization-controlled two-dimensional experiments are outlined in Sec. II, followed by a discussion of the results.

II. EXPERIMENTS

A. All-parallel polarization two-dimensional spectroscopy

The principles and interpretation of two-dimensional spectroscopy experiments have been reviewed in Refs. 47 and 48. Briefly, a sequence of three excitation pulses resonantly interact with the electronic states of the sample in a non-collinear geometry. Interaction with the first pulse causes the optical response to evolve as a coherence between the ground and excited states for the coherence time, τ. Following the second pulse, the system relaxes during the waiting time T, where excited state dynamics and ground state bleaching signatures can be monitored. The final pulse stimulates the emission of a signal field in the phased matched direction $\mathbf{k}_s = -\mathbf{k}_1 + \mathbf{k}_2 + \mathbf{k}_3$ during the rephasing time t, where $\mathbf{k}_i$ indicates the wave vector of the ith field. A reference pulse is co-propagated with the signal and interferes with the signal in a grating spectrometer. The resultant interferogram is measured on a charge coupled device. Following apodization, a two-dimensional Fourier transform of the data over the coherence time and rephasing time axes generates two-dimensional maps as a function of the waiting time.[49] Simply interpreted, these maps correlate absorption events along the ω_τ axis with emission events on the ω_t axis for each waiting time. Relaxation and energy transfer dynamics can be monitored by monitoring the changes in spectral features of the correlation maps with waiting time.

All experiments were conducted utilizing the gradient assisted photon echo spectrometer (GRAPE), which has been described in detail in Refs. 50 and 51. The GRAPE spectrometer only acquires the rephasing portion of the optical response. The output of a regenerative amplifier was focused into argon gas at ~1.3 atm, generating a spectrally broadened output pulse centered near 800 nm with ~90 nm full width at half maximum of bandwidth. The spectrum of the resultant pulse is shown in Figure 1. Our laser source does not produce sufficient bandwidth to fully capture the red side of the 850 nm band; therefore, our experiment cannot probe the dynamics of some low energy states. Furthermore, the shape of the laser pulse distorts the position of the 850 nm band toward 835 nm. The broadened pulse was compressed utilizing a spatial light modulator based pulse shaper (Biophotonics Solutions) to a nearly transform-limited 15 fs full width at half maximum, as confirmed through a multiphoton intrapulse

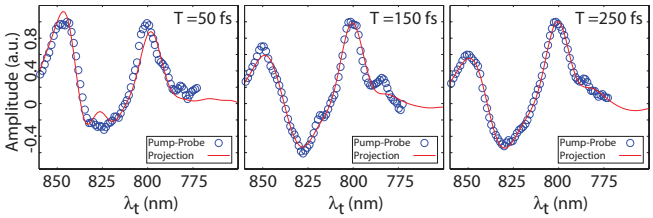

FIG. 2. Comparison of the projection of the two-dimensional spectra onto the λ_t axis with the separately acquired spectrally resolved transient absorption data for the indicated waiting times.

interference phase scan (MIIPS) and separately measured transient grating frequency resolved optical gating measurements (TG-FROG), both conducted at the sample position.[52,53] Due to uncertainties in the timings between the excitation pulses and local oscillator, as well as differing carrier envelope phases and compression, the absolute phase of the measured signal is not precisely known.[54,55] These uncertainties lead the real and imaginary portions of the signal to become mixed. The real portion of the signal is recovered by phasing the data with the following phase factor:

$$\Phi_o + (\omega_\tau - \omega_o)\,\tau_c + (\omega_t - \omega_o)\,t_c + (\omega_t - \omega_o)^2\,t_q^2.$$

Here, Φ_o is a constant phase factor, τ_c corrects for error in the measured timings between the first two pulses, t_c corrects for error in the measured timing between the third pulse and the signal, and t_q corrects for pulse chirp and unequal dispersion present in the interferometer. The dispersion in the optical setup most likely arises from the extra neutral density in the path of the local oscillator, which is used to match the local oscillator intensity to the signal intensity, maximizing the fringe contrast of the acquired interferogram. The four fitting parameters are then adjusted to match the projection of the two-dimensional spectra onto the ω_t axis with separately acquired spectrally resolved pump probe data, shown in Figure 2.[55] The timings between beams were determined through spectra Interferometry.[56] Data analysis proceeded as previously described.[49,51]

The LH2 complex was isolated and purified from cultures of *Rhodobacter sphaeroides* following the procedures described by Frank *et al.*[57] An additional purification step though a DEAE-Sepharose column eluted with 500 mM NaCl isolated only the LH2 complexes. The sample was concentrated to an optical density of ~0.2 at 800 nm in a 200 μm flow cell. All experiments were conducted at the ambient temperature of 294 K. The pulse energy was 140 nJ per pulse for the three excitation pulses, resulting in a flux of 42 μJ/cm^2, which is similar to the flux in point-by-point two-dimensional spectrometers and low enough to remain in the single exciton regime.[51,58,59]

B. Dynamics polarization sequence

To probe the initial energy transfer events in LH2 we have utilized a polarization sequence which highlights the initial energy transfer events. The polarization scheme relies on the same wave vector dependence between pulses two and three in a two-dimensional experiment.[36] At a waiting time of zero the response is invariant to the exchange between the second and third pulses, resulting in the polarization response of the pulse polarization sequences XXYY and XYXY to be identical for zero waiting time. Here, the polarization of the three pump beams and resultant signal are given in order from left to right (1,2,3,LO). The waiting time dependence of the difference between these two polarization sequences, XXYY – XYXY, will then highlight purely dynamical processes that occur during the waiting time that break this symmetry. The waiting time dependence of traces through the two-dimensional plots will then directly reveal the time scales of the energy transfer dynamics while eliminating contributions from static populations. This polarization sequence can be encoded into a single pulse sequence[41] given by $-\pi/2$, $-\pi/3$, $\pi/3$,0, where the angle of the polarization of the three pump pulses and signal relative to the y-axis is given in radians. A single polarization sequence scheme of this form avoids taking the difference between two large signals and increases the signal-to-noise relative to two separate experiments.[41] The polarization was controlled through the inclusion of three true zeroth-order half wave plates that were placed in the beam paths of the three pump beams. The polarization was calibrated relative to the local oscillator with a Glan-Thompson polarizer placed at the sample position. We estimate the error in our polarizations to be less than 0.02 radians (1°). The waiting time was sampled from 0 fs to 1000 fs in 10 fs steps. All other experimental conditions were identical to the all-parallel polarization data. Only the absolute values of the polarized controlled spectra are reported due to uncertainties in the global phase.

III. RESULTS AND DISCUSSION

The all-parallel polarization data are shown in Figure 3. The early waiting time shows a rapid 100 fs decay in the 850 nm region alongside equilibration among the states within the 800 nm region. The ultrafast initial decay in the 850 nm region has been previously observed in transient absorption measurements and has been attributed to relaxation to the lowest excited state in the LH2 ring as well as a collapse in the coherence length of the exciton.[14,16,60] Concurrently with the decrease in intensity of the 850 nm diagonal feature, we observe a downward shift of 110 cm^{-1} occurring on a 400 fs time scale. No appreciable shift is detected within the 800 nm band. The lack of a shift in the 800 nm band agrees with photon echo peak shift experiments which revealed that the B800 pigments are more weakly coupled to the protein environment than the B850 pigments.[18,61] The weaker pigment bath coupling results in a smaller shift and also manifests in the different single molecule fluorescence excitation spectral line widths.[15]

A cross peak becomes evident within the 800 nm band, reflecting downhill energy transfer on a 100 fs timescale. This cross peak connects the weak absorbance around 750–775 nm, which results from higher lying excitations of the B850 chromophores, with the main peak at 800 nm. Due to the relatively strong intensity of the cross-peak when compared to the diagonal peak in the 750–775 nm, we attribute this peak to energy transfer from B850* states into B800 states

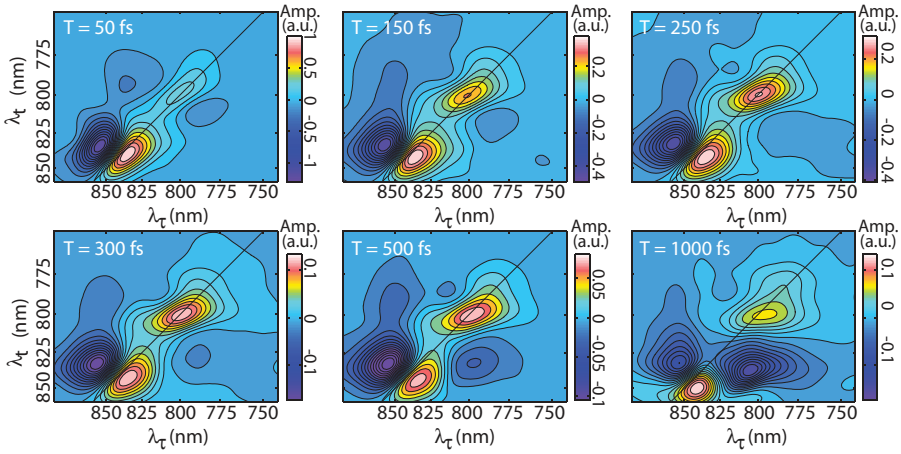

FIG. 3. Phased two-dimensional spectra at waiting times of 50 fs, 150 fs, and 250 fs, reveal the fast intra-band relaxation in the 800 nm region of the spectrum, which is resolved as a cross peak which grows in with increasing waiting time. A cross peak connecting the two bands grows in on a slower 600 fs timescale, shown in the waiting time of 300 fs, 500 fs, and 1000 fs maps.

or states of mixed character with a larger transition dipole moment. The cross peak provides direct experimental evidence of inter-band energy transfer within the 800 nm band which has been proven difficult to resolve with transient absorption measurements. Interestingly, this energy transfer pathway, B850*–B800–B850, results in a cyclical motion of the exciton in space. Concurrent with the energy transfer within the 800 nm region is a transfer of excitation between the two rings on a slower ∼700 fs time scale, which is reflected by the cross peak between the 800 nm and 850 nm bands appearing on a longer time scale. The cross peak is dominated by the growth in an excited state absorption feature at higher energies and a stimulated emission signal at lower energies at the edge of our bandwidth in the emission axis (λ_t axis). Due to incomplete overlap of the spectrum of our laser pulse with the 850 nm absorption feature, the maximal cross peak intensity is located at $\lambda_t = 835$ nm. This apparent change is an artifact arising from the pulse spectrum. The energy transfer cross peak extends to the blue edge of our bandwidth in the λ_τ dimension, connecting the 770 nm diagonal with the 835 nm diagonal feature. The blue edge of the cross peak reflects intra-band B850*–B850 energy transfer. The energy transfer time scale between the 800 nm and 850 nm bands is ∼700 fs, in good agreement with previous two-color transient absorption experiments.[23] The relaxation process is completed after 1000 fs and the two-dimensional spectra for subsequent waiting times are indistinguishable.

The two-dimensional spectra closely resemble the two dimensional spectra of the related B800–B820 complex (LH3) from *Rhodopseudomonas acidophila* which were conducted at 77 K.[62] Two dimensional spectra of the B800–B820 complex revealed two strong features on the diagonal corresponding to the main transition in the near infrared and large excited state absorption features above the diagonal.[62] The B800–B820 complex is a naturally occurring variant of the LH2 complex in which minor modifications of the pigment-protein interactions of the 18 strongly interacting chromophores blueshifts the lower energy absorption band from 850 nm to 820 nm.[63] The intra-band energy transfer event observed in the B850–B800 LH2 studied here was not resolved in the previous two-dimensional measurements on the B800–B820 complex. We attribute this discrepancy to the broader bandwidth of our excitation pulses when comparing our experimental conditions to theirs, which allow for the high energy tail corresponding to B850* excitations to be probed. Different electronic properties of the two light harvesting complexes and the different temperatures could also potentially explain the discrepancy. Within a simple Redfield formalism, the rate of energy transfer between two states can be expressed by the following equation:

$$K_{i\to j} = J_{ij}[(1 + n(\omega_{ij}))\rho(\omega_{ij}) + \rho(\omega_{ji})n(\omega_{ji})].$$

Here $n(\omega_{ij})$ is the Bose-Einstein distribution evaluated at the energy difference between the excitons, ω_{ij}; $\rho(\omega_{ij})$ is the spectral density evaluated at the same point, and J_{ij} is the spatial overlap of the excitons i and j.[64] Assuming the spectral density and electronic couplings are temperature independent, the temperature dependence will be determined by changes in the equilibrium population of phonons. Thus, transfer rates between states with smaller energy differences, i.e., smaller ω_{ij}, depend more strongly on temperature than rates between states with larger gaps. Hence, the rate of intra-band transitions changes more rapidly with temperature than the inter-band transition rates, changing the relative branching ratios and suppressing the strength of the intra-band cross peak. The changes in the protein residues in the B800–B820 complex could potentially induce changes in the spectral density, which would also change the relative branching ratios. It is unclear which effect explains the observed difference. Besides the lack of an intra-band cross peak, the spectra and corresponding dynamics, including the negative sign of the energy transfer cross peak between the bands, are quite similar, indicating the electronic structure and dynamics of the two complexes are closely analogous.

The polarization sequence that highlights the excited state dynamics ($-\pi/2$, $-\pi/3$, $\pi/3$, 0) shows different dynamics during the first hundred femtoseconds than the all-parallel polarization experiments. To coarsely examine the time scales of the energy transfer events, we integrate the magnitude of the signal field over both frequency axes to

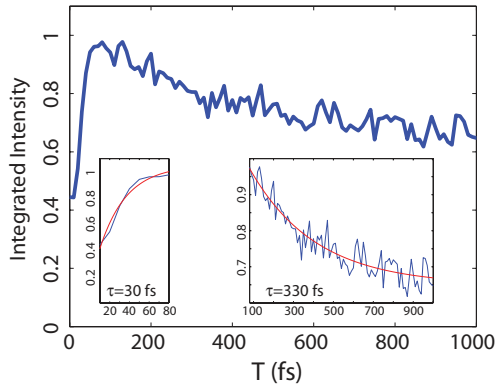

FIG. 4. Plot of the integrated magnitude of the excited state dynamics polarization sequence signal as a function of the waiting time. The signal shows a 30 fs rise time before decaying on a slower 330 fs time scale to a constant value. The residual signal present at a waiting time of 0 fs results from polarization errors and the evolution of the system within the finite pulse width. The inset plots show a single exponential fit (red) to the initial rise and decay from the maximal value located at 80 fs.

give an absolute signal strength as a function of waiting time. The time scales of this integrated signal reflect the dominant energy transfer time scales contributing to the signal. The integrated signal also provides a simple diagnostic test of the validity of the polarization scheme. A plot of the integrated signal magnitude is shown in Figure 4. At a waiting time of 0 fs, the signal is strongly suppressed and rapidly grows in on a 30 fs time scale to reach a maximal value at a waiting time of 80 fs. The intensity of the signal at T = 0 fs is between 20% and 40% of the maximal value, depending on the alignment; we attribute this residual signal to polarization errors as well as system evolution during the laser pulse. The rapid growth in signal is followed by a slower decay on a 330 fs time scale to a final intensity of 65% of the maximal intensity. Both the initial rise and subsequent fall in signal intensity are well modeled by a single exponential. These results confirm our expectation for the signal: Close to zero intensity at early waiting times followed by a rise in the signal reflecting the energy transfer time scales present in the system.

Two-dimensional spectra using the excited state polarization sequence are shown in Figure 5. Due to uncertainty regarding the absolute phase of the signal, we report only the magnitude of the signal field. The early waiting spectra (T < 80 fs), corresponding to the top panel of Figure 5, reveal that the strongest response appears mostly on the diagonal in the 850 nm region. A cross peak connecting the 800 nm diagonal with the 834 nm diagonal is also observed at very early waiting times. We interpret the cross peak feature as arising from B850* to B850 energy transfer. Due to the strong coupling between chromophores in the B850 ring, the resultant dynamics of energy transfer from the B850* to B850 has been predicted to be sub 100 fs and is in agreement with our measurements.[19] In the earliest two waiting times displayed, a cut through the λ_τ dimension shows unusually low intensity of the cross peak at 800 nm. This reduction in signal amplitude around $\lambda_\tau = 800$ nm most likely reflects the underlying electronic structure of the 800 nm absorption feature. Polarization controlled single molecule experiments have revealed that the 850 nm band is mostly comprised of two electronic states.[15] Detailed modeling of the single molecule data suggests that a third electric state with weaker dipole moment is additionally contributing to the experimental results.[65] The two main electronic states are typically referred to as k = ±1 states, in reference to the solutions for a particle on a ring.[66,67] The inclusion of disorder induced through protein conformational changes complicates this picture but the simple model remains useful, particularly for nonlinear ensemble experiments. Calculations have shown that the transition dipole moments for higher lying k states are only ∼20% of the strength of those for a single bacteriochlorophyll.[19] These states contribute appreciably to the absorption spectrum, and are responsible for the high energy tail at 770 nm shown in

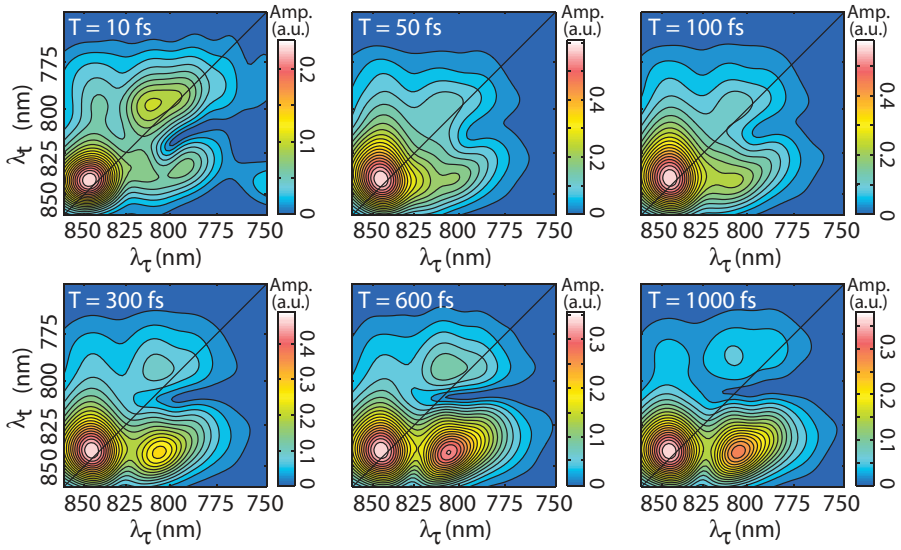

FIG. 5. Excited state dynamics 2D spectra for waiting times of 10 fs, 50 fs, and 100 fs reveal an ultrafast energy transfer component between the two absorption bands, which is assigned to B850*–B850 energy transfer. Later waiting time spectra at 300 fs, 600 fs, and 1000 fs show the slower energy transfer time scales arising from B800–B850 transfer.

Figure 1.[5,19,20] However, the third order response scales as the dipole moment to the fourth power, which strongly suppresses contributions to the response from higher lying k states. This effect can be seen in the all-parallel polarization data shown in Figure 3, in which the diagonal peak that corresponds to the high energy tail comprised of B850* is strongly suppressed relative to the main diagonal peaks. However, cross peaks involving the B850* states can be enhanced by the larger transition dipole of the acceptor state, permitting their detection. Evidence for a third electronic state in ensemble hole burning experiments suggests the lowest energy state lies predominantly at 870 nm, well outside the bandwidth of our laser pulse.[68] We interpret the reduction in the amplitude of the cross-peak near $\lambda_\tau = 800$ as arising from a decreased density of states of B850* around 800 nm. The same conclusion was reached in modeling of transient absorption experiments conducted on the 800 nm band.[19,26] These calculations reveal heterogeneity in the decay of the bleaching signal as a function of the excitation wavelength, with a minimal decay rate at 800 nm.[19,26] The later waiting time spectra in Figure 5 show that the diagonal 800 nm feature continues to lose intensity concurrent with the growth of the lower cross peak connecting the two bands. The upper cross peak feature most likely arises from excited state absorption, much like it does in the all-parallel polarization data shown in Figure 4.

Traces through different regions of the excited state polarization two-dimensional maps provide a more detailed picture of the dynamics and are shown in Figure 6. In general, the traces show an initial rise followed by a slow decay or rise to a long time value. The 800 nm diagonal feature decays on an 825 fs time scale, approximately matching the time scale of the cross peak dynamics in the all-parallel polarization. The diagonal feature at 770 nm, which corresponds to

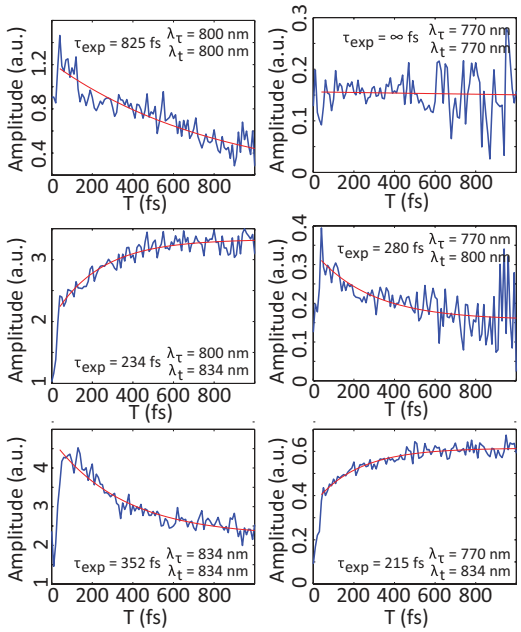

FIG. 6. Traces through waiting time through various regions of the excited state 2D spectrum reveal the varied population dynamics. Traces show a sharp rise from zero waiting time and peak at a waiting time of around 80 fs, and then undergo slower relaxation dynamics.

B850* sates, is too weak to measure the population loss conclusively. Cross peaks connecting the 770 nm absorption to emission at 800 nm and 834 nm show time scales on the order of 200 fs, indicating that population in the B850* states most likely persists on this timescale. The cross peak amplitude is enhanced by the large dipole strength of the states in the 800 nm and 850 nm region permitting their measurement. The diagonal 834 nm feature, corresponding to the B850 states, decays on a 350 fs time scale, reflecting relaxation to the fluorescent state. The cross peak connecting the 800 nm and 834 nm regions shows a fast 234 fs growth component; our data do not have sufficient signal-to-noise to resolve the 700 fs growth found in previous pump probe experiments and the all-parallel polarization two-dimensional experiments.[22,23] The 234 fs growth component most likely reflects B850* to B850 transfer. Within a Redfield picture, these B850* states lack the spatial overlap characteristics of the other B850* states responsible for the faster relaxation dynamics. This difference helps to explain why some B850* states contribute to the rapid growth in the first 80 fs while others do not. The slower 700 fs component is most likely also present and is simply undetected due to experimental noise. Alternatively, the polarization used here requires that orientation of the transition dipole moments between different states are non-parallel. Hence, if the transition dipole moments of the B800 states are parallel to the B850 states, then the energy transfer cross peak would not contribute to the signal.

Currently, the most complete theoretical description of the energy transfer dynamics in LH2 has been provided in a study by Novoderezhkin and co-workers.[19] This work utilizes a non-secular Redfield model to simultaneously reproduce the linear absorption spectrum and wavelength dependent isotropic and anisotropic transient absorption experiments. The transient absorption experiments performed by Wendling and co-workers were conducted with relatively narrow band pulses that were tuned across the 800 nm band with the pump and probe wavelengths being identical.[26] The simultaneous fitting of the experimental data constrains the model, permitting a confident assignment of all energy transfer timescales in the LH2 complex. These calculations model experiments conducted at 77 K on LH2 from *Rhodospirillum molischianum*. Therefore, we do not expect our results to completely agree with their predictions due to the large differences in temperature and inter-chromophoric couplings between our samples (the decreased ring size in *Rhodospirillum molischianum* induces stronger coupling). For example, the average time scale for energy transfer from 800 nm to 850 nm at 77 K in *Rhodobacter sphaeroides* is 1.2 ps, which is slower than the 1 ps time scale in *Rhodospirillum molischianum*.[26,29] Overall, our findings are largely consistent with the model of Novoderezhkin and co-workers. Their model predicts that the B800–B800 energy transfer time scale was sufficiently slow to not appreciably contribute to the relaxation dynamics. Our results are consistent with this prediction, as no cross peak is detected connecting the 800 nm diagonal feature with lower energy states in the 800 nm band. Furthermore, the rapid dynamics of the B850* to B850 relaxation are also evident in our measurements. Their model predicts a large range of energy transfer time scales for the B850* to B800 transfer,

ranging from 60 to 200 fs, which is also manifested in our experiments. Some discrepancies exist between Novoderezhkin *et al.*'s model and our experimental results. They found that a B800–B850*–B850 pathway was nearly the same intensity as the direct B800–B850 relaxation. Such signals are difficult to resolve because the B800 and B850* states involved in the energy transfer process lie close in energy to each other, and if present, they also appear to have parallel transition dipoles because our measurements do not show any signals characteristic of this process (i.e., a cross peak or 800 nm diagonal peak). Similarly, we do not see appreciable signal for the reverse process, B850* to B800 transfer. In their model this pathway of energy relaxation was significantly slower, occurring on a time scale greater than 250 fs. The dynamics of the B850 relaxation are also significantly different. In the bandwidth accessible with our laser source, the predicted time scales of relaxation are on the order of 40–70 fs. While we do observe a rapid decay component on this time scale, additional slower components are also present in the B850 diagonal peak. The shift of the 850 nm feature may not be readily modeled with Redfield theory because Redfield theory assumes that the phonons are always in an equilibrium configuration.[69]

IV. CONCLUSION

Two-dimensional spectroscopy is well suited to measurements of inter-band and intra-band energy transfer events that can be challenging to access with transient absorption spectroscopy due to the closely lying resonances and the inherit tradeoff between spectral selectively and temporal resolution. For example, in the experiments by Wendling and co-workers, pulse lengths of ∼130 fs were required in order to probe the excitation dependent relaxation dynamics. The longer pulse lengths and subsequent coherent artifact in transient absorption experiments made the experiments less sensitive to some rapid energy transfer events. Two-dimensional methodologies provide simultaneous high temporal and spectral resolution and the ability to separate energy transfer events into cross-peaks.

Excitation energy transfer events in the LH2 complex are investigated with both all-parallel polarization two-dimensional electronic spectroscopy and a polarization sequence designed to reveal the initial excitation energy transfer events. The phased all-parallel polarization data reveal time scales of energy transfer in LH2 in good agreement with previous measurements. Qualitatively, the peak shape and spectral features in the two-dimensional maps are largely consistent with previous two-dimensional experiments on the related B800–B820 mutant, indicating that the electronic structure of the two complexes is quite similar. An additional decay channel of energy transfer from the higher lying excitations of the B850 pigments into states in the 800 nm band was resolved as a cross peak in the 800 nm region. A polarization sequence that highlights the initial events of energy transfer reveals an ultrafast energy transfer cross peak between the 800 nm and 850 nm diagonal features that was not resolvable in the all-parallel polarization data. We attribute this ultrafast energy transfer component to relaxation from B850* states into B850 states. Taken together the measurements are in good agreement with calculations by Novoderezhkin and co-workers and provide direct experimental evidence for energy transfer processes that were previously inferred from calculations.[19] The excited state polarization sequence is generally applicable to systems with dipole transitions and can provide additional information on the time scales of excitation migration in spectrally congested systems.

ACKNOWLEDGMENTS

The authors would like to thank National Science Foundation (NSF) Materials Research Science and Engineering Center (MRSEC) (DMR 08-02054), AFOSR (FA9550-09-1-0117), the Defense Advanced Research Projects Agency (DARPA) QuBE program (N66001-10-1-4060), and the Searle Foundation for partially supporting this work. A.F.F. and P.D.L. acknowledge support from the DOE SCGF program. P.D.D. was supported by the Graduate Program in Biophysical Sciences at the University of Chicago (National Institutes of Health Grant No. T32 EB009412).

[1] H. van Amerongen, L. Valkunas, and R. van Grondelle, *Photosynthetic Excitons* (World Scientific, Singapore, 2000).
[2] B. R. Green and W. W. Parson, *Light-Harvesting Antennas* (Kluwer Academic Press, Dordrecht, 2001).
[3] R. Blankenship, *Molecular Mechanisms of Photosynthesis* (Blackwell Science, Oxford, 2002).
[4] G. McDermott, S. M. Prince, A. A. Freer, A. M. Hawthornthwaitelawless, M. Z. Papiz, R. J. Cogdell, and N. W. Isaacs, Nature (London) **374**, 517 (1995).
[5] M. H. C. Koolhaas, R. N. Frese, G. J. S. Fowler, T. S. Bibby, S. Georgakopoulou, G. van der Zwan, C. N. Hunter, and R. van Grondelle, Biochemistry **37**, 4693 (1998).
[6] A. Angerhofer, R. J. Cogdell, and M. F. Hipkins, Biochim. Biophys. Acta **848**, 333 (1986).
[7] J. Koepke, X. C. Hu, C. Muenke, K. Schulten, and H. Michel, Structure **4**, 581 (1996).
[8] S. Georgakopoulou, R. N. Frese, E. Johnson, C. Koolhaas, R. J. Cogdell, R. van Grondelle, and G. van der Zwan, Biophys. J. **82**, 2184 (2002).
[9] V. Sundstrom, T. Pullerits, and R. van Grondelle, J. Phys. Chem. B **103**, 2327 (1999).
[10] X. C. Hu, T. Ritz, A. Damjanovic, F. Autenrieth, and K. Schulten, Q. Rev. Biophys **35**, 1 (2002).
[11] R. J. Cogdell, A. Gall, and J. Kohler, Q. Rev. Biophys **39**, 227 (2006).
[12] R. van Grondelle and V. I. Novoderezhkin, Phys. Chem. Chem. Phys. **8**, 793 (2006).
[13] R. Monshouwer, M. Abrahamsson, F. van Mourik, and R. van Grondelle, J. Phys. Chem. B **101**, 7241 (1997).
[14] M. Chachisvilis, O. Kuhn, T. Pullerits, and V. Sundstrom, J. Phys. Chem. B **101**, 7275 (1997).
[15] A. M. van Oijen, M. Ketelaars, J. Kohler, T. J. Aartsma, and J. Schmidt, Science **285**, 400 (1999).
[16] L. D. Book, A. E. Ostafin, N. Ponomarenko, J. R. Norris, and N. F. Scherer, J. Phys. Chem. B **104**, 8295 (2000).
[17] B. P. Krueger, G. D. Scholes, and G. R. Fleming, J. Phys. Chem. B **102**, 5378 (1998).
[18] T. H. Joo, Y. W. Jia, J. Y. Yu, D. M. Jonas, and G. R. Fleming, J. Phys. Chem. **100**, 2399 (1996).
[19] V. Novoderezhkin, M. Wendling, and R. van Grondelle, J. Phys. Chem. B **107**, 11534 (2003).
[20] A. F. Fidler, V. P. Singh, P. D. Long, P. D. Dahlberg, and G. S. Engel, J. Phys. Chem. Lett. **4**, 1404 (2013).
[21] R. Hildner, D. Brinks, J. B. Nieder, R. J. Cogdell, and N. F. van Hulst, Science **340**, 1448 (2013).
[22] S. Hess, F. Feldchtein, A. Babin, I. Nurgaleev, T. Pullerits, A. Sergeev, and V. Sundstrom, Chem. Phys. Lett. **216**, 247 (1993).
[23] A. P. Shreve, J. K. Trautman, H. A. Frank, T. G. Owens, and A. C. Albrecht, Biochim. Biophys. Acta **1058**, 280 (1991).

[24]B. P. Krueger, G. D. Scholes, R. Jimenez, and G. R. Fleming, J. Phys. Chem. B **102**, 2284 (1998).
[25]E. E. Ostroumov, R. M. Mulvaney, R. J. Cogdell, and G. D. Scholes, Science **340**, 52 (2013).
[26]M. Wendling, F. van Mourik, I. H. M. van Stokkum, J. M. Salverda, H. Michel, and R. van Grondelle, Biophys. J. **84**, 440 (2003).
[27]H. van der Laan, T. Schmidt, R. W. Visschers, K. J. Visscher, R. van Grondelle, and S. Volker, Chem. Phys. Lett. **170**, 231 (1990).
[28]N. R. S. Reddy, G. J. Small, M. Seibert, and R. Picorel, Chem. Phys. Lett. **181**, 391 (1991).
[29]R. Monshouwer, I. O. Dezarate, F. Vanmourik, and R. Vangrondelle, Chem. Phys. Lett. **246**, 341 (1995).
[30]T. Pullerits, S. Hess, J. L. Herek, and V. Sundstrom, J. Phys. Chem. B **101**, 10560 (1997).
[31]Y. Z. Ma, R. J. Cogdell, and T. Gillbro, J. Phys. Chem. B **101**, 1087 (1997).
[32]J. M. Salverda, F. van Mourik, G. van der Zwan, and R. van Grondelle, J. Phys. Chem. B **104**, 11395 (2000).
[33]T. Brixner, J. Stenger, H. M. Vaswani, M. Cho, R. E. Blankenship, and G. R. Fleming, Nature (London) **434**, 625 (2005).
[34]J. Dostal, T. Mancal, R. Augulis, F. Vacha, J. Psencik, and D. Zigmantas, J. Am. Chem. Soc. **134**, 11611 (2012).
[35]J. M. Anna, E. E. Ostroumov, K. Maghlaoui, J. Barber, and G. D. Scholes, J. Phys. Chem. Lett. **3**, 3677 (2012).
[36]D. Abramavicius, D. V. Voronine, and S. Mukamel, Biophys. J. **94**, 3613 (2008).
[37]R. M. Hochstrasser, Chem. Phys. **266**, 273 (2001).
[38]E. L. Read, G. S. Engel, T. R. Calhoun, T. Mancal, T. K. Ahn, R. E. Blankenship, and G. R. Fleming, Proc. Natl. Acad. Sci. U.S.A. **104**, 14203 (2007).
[39]E. L. Read, G. S. Schlau-Cohen, G. S. Engel, J. Z. Wen, R. E. Blankenship, and G. R. Fleming, Biophys. J. **95**, 847 (2008).
[40]G. S. Schlau-Cohen, E. De Re, R. J. Cogdell, and G. R. Fleming, J. Phys. Chem. Lett. **3**, 2487 (2012).
[41]M. T. Zanni, N. H. Ge, Y. S. Kim, and R. M. Hochstrasser, Proc. Natl. Acad. Sci. U.S.A. **98**, 11265 (2001).
[42]E. L. Read, G. S. Schlau-Cohen, G. S. Engel, T. Georgiou, M. Z. Papiz, and G. R. Fleming, J. Phys. Chem. B **113**, 6495 (2009).
[43]G. S. Schlau-Cohen, T. R. Calhoun, N. S. Ginsberg, M. Ballottari, R. Bassi, and G. R. Fleming, Proc. Natl. Acad. Sci. U.S.A. **107**, 13276 (2010).
[44]N. S. Ginsberg, J. A. Davis, M. Ballottari, Y. C. Cheng, R. Bassi, and G. R. Fleming, Proc. Natl. Acad. Sci. U.S.A. **108**, 3848 (2011).
[45]G. S. Schlau-Cohen, A. Ishizaki, T. R. Calhoun, N. S. Ginsberg, M. Ballottari, R. Bassi, and G. R. Fleming, Nat. Chem. **4**, 389 (2012).
[46]S. Westenhoff, D. Palecek, P. Edlund, P. Smith, and D. Zigmantas, J. Am. Chem. Soc. **134**, 16484 (2012).
[47]M. H. Cho, Chem. Rev. **108**, 1331 (2008).
[48]D. M. Jonas, Annu. Rev. Phys. Chem. **54**, 425 (2003).
[49]T. Brixner, T. Mancal, I. V. Stiopkin, and G. R. Fleming, J. Chem. Phys. **121**, 4221 (2004).
[50]E. Harel, A. F. Fidler, and G. S. Engel, Proc. Natl. Acad. Sci. U.S.A. **107**, 16444 (2010).
[51]E. Harel, A. F. Fidler, and G. S. Engel, J. Phys. Chem. A **115**, 3787 (2011).
[52]V. V. Lozovoy, I. Pastirk, and M. Dantus, Opt. Lett. **29**, 775 (2004).
[53]J. N. Sweetser, D. N. Fittinghoff, and R. Trebino, Opt. Lett. **22**, 519 (1997).
[54]A. W. Albrecht, J. D. Hybl, S. M. G. Faeder, and D. M. Jonas, J. Chem. Phys. **111**, 10934 (1999).
[55]J. D. Hybl, A. A. Ferro, and D. M. Jonas, J. Chem. Phys. **115**, 6606 (2001).
[56]L. Lepetit, G. Cheriaux, and M. Joffre, J. Opt. Soc. Am. B **12**, 2467 (1995).
[57]H. A. Frank, B. W. Chadwick, J. J. Oh, D. Gust, T. A. Moore, P. A. Liddell, A. L. Moore, L. R. Makings, and R. J. Cogdell, Biochim. Biophys. Acta **892**, 253 (1987).
[58]J. D. Hybl, A. W. Albrecht, S. M. G. Faeder, and D. M. Jonas, Chem. Phys. Lett. **297**, 307 (1998).
[59]M. L. Cowan, J. P. Ogilvie, and R. J. D. Miller, Chem. Phys. Lett. **386**, 184 (2004).
[60]V. Nagarajan, R. G. Alden, J. C. Williams, and W. W. Parson, Proc. Natl. Acad. Sci. U.S.A. **93**, 13774 (1996).
[61]R. Jimenez, F. vanMourik, J. Y. Yu, and G. R. Fleming, J. Phys. Chem. B **101**, 7350 (1997).
[62]D. Zigmantas, E. L. Read, T. Mancal, T. Brixner, A. T. Gardiner, R. J. Cogdell, and G. R. Fleming, Proc. Natl. Acad. Sci. U.S.A. **103**, 12672 (2006).
[63]K. McLuskey, S. M. Prince, R. J. Cogdell, and N. W. Isaacs, Biochemistry **40**, 8783 (2001).
[64]A. G. Redfield, IBM J. Res. Dev. **1**, 19 (1957).
[65]S. J. Jang, R. J. Silbey, R. Kunz, C. Hofmann, and J. Kohler, J. Phys. Chem. B **115**, 12947 (2011).
[66]V. I. Novoderezhkin and A. P. Razjivin, Biophys. J. **68**, 1089 (1995).
[67]T. Meier, Y. Zhao, V. Chernyak, and S. Mukamel, J. Chem. Phys. **107**, 3876 (1997).
[68]H. M. Wu, N. R. S. Reddy, and G. J. Small, J. Phys. Chem. B **101**, 651 (1997).
[69]A. Ishizaki and G. R. Fleming, J. Chem. Phys. **130**, 234110 (2009).